

# Role of *microRNA-122* in hepatic lipid metabolism of the weanling female rat offspring exposed to prenatal and postnatal caloric restriction☆

Yun Dai, Shubhamoy Ghosh, Bo-Chul Shin, Sherin U. Devaskar\*

Department of Pediatrics and the Children's Discovery and Innovation Institute, David Geffen School of Medicine UCLA, Los Angeles, CA

Received 21 December 2018; received in revised form 23 June 2019; accepted 30 July 2019

## Abstract

We examined the role of hepatocyte *microRNA-122* and hypothalamic neuropeptides, in weanling (21d) female rats exposed to calorie restriction induced growth restriction either prenatally (IUGR), postnatally (PNGR) or both (IPGR) vs. ad lib fed controls (CON). IUGR were hyperinsulinemic, hyperleptinemic and dyslipidemic with high circulating *miR-122*. In contrast, PNGR and IPGR displayed insufficient glucose, insulin and leptin amidst high ketones with a dichotomy in circulating *miR-122* of PNGR < IPGR = CON. Examination of livers revealed a reduction in *miR-122* expression in PNGR and IPGR reflecting the hepatic size. This reduction of hepatic *miR-122* was associated with an increase in specific target transcripts (ALDO-A, BCKDK, PPAR-β) and those mediating fatty acid oxidation (PGC-1α, CPT-1α), with a concomitant suppression of fatty acid and cholesterol synthesizing transcripts (FAS, HMGCR). Functionally, these changes correlated with increased fatty acid oxidation and mitochondrial CPT1α enzyme activity *ex vivo*. In vitro physiologic (serum starvation) and genetic manipulation of *miR-122* in H4IIE hepatoma cells revealed fidelity in regulating ALDO-A/BCKDK, but an infidelity in perturbing fatty acid/cholesterol synthesizing and oxidizing gene transcripts. Nevertheless, changes in endogenous *miR-122* maintained singular directionality while altering FAS/HMGCR and CPT-1α/PGC-1α, almost reflecting each other, and thereby maintaining a balance in fatty acid/cholesterol supply necessary to meet the in vitro demands of these rapidly proliferating transformed cells. Successive microarray based analysis, comparing IPGR to CON demonstrated differential expression of hypothalamic genes mediating cell proliferation and survival, appetite/energy balance, circadian rhythm and obesity/diabetes. We conclude that *miR-122* regulates genes mediating fatty acid/cholesterol metabolism in postnatal female rats, fueling the energy demand.

Published by Elsevier Inc.

**Keywords:** Intra-uterine growth restriction; *microRNA-122*; Hepatic fatty acid synthesis; Fatty acid oxidation; Hypothalamic genes; Energy balance; Circadian rhythm

## 1. Introduction

Unbalanced nutrition is a major cause for metabolic associated maladies. Occurrence of overweight among the children of developed countries and its association with type II diabetes mellitus and other metabolic syndromes implies a combination of factors, majority of which bear connections with nutritional intake during different phases of the life cycle [1]. The relevance of nutrition during pregnancy and early infancy in defining long-term effects on health and survival has been described earlier [2]. The Developmental Origins of Health and Disease (DOHaD) paradigm also provides a framework to assess the effect of early nutrition and growth on long-term health. This body of literature shows that early nutrition has significant consequences on later health and well-being [3–7].

Consistent with DOHaD, altered glucose and lipid metabolism with various metabolic maladies occur in animal models of prenatal caloric restriction. These dysregulations include fatty liver, increased hepatic cholesterol concentrations, upregulation of lipogenic genes [8] and

downregulation of transcription factors like PPARα and PPARγ [9]. Increased lipogenesis may contribute to the increased adiposity in adult IUGR animal models, but also in children and human adults. In contrast, postnatal calorie and protein restriction or delayed “catch up growth” reversed development of obesity in IUGR animal models [10]. Reduction of fat mass and body weight was observed in maternal calorie restricted offspring exposed to postnatal calorie restriction in mice [11] and rats [12,13]. Differential changes in glucose and fatty acid synthesizing regulatory genes such as hepatic fatty acid synthase (FAS), Sterol Regulatory Element Binding Protein 1c (SREBP-1c) and Phosphoenolpyruvate Carboxykinase (PEPCK) were noted at the adult stage [14]. However, the underlying mechanisms that alter transcription factors or genes that regulate triglycerides (TG), cholesterol and fatty acid homeostasis in the offspring, exposed to either prenatal or postnatal calorie restriction, have not been investigated at an early stage in life. Such changes if present early in life would provide credence to the concept of persistent changes in the adult offspring in response to early life events.

☆ The authors have no conflicts of interest. This work was supported by grants from the National Institutes of Health HD-41230 and HD-81206 (to SUD).

\* Corresponding author at: 10833 Le Conte Avenue, MDCC-22-412, Los Angeles, CA 90095-1752. Tel.: +1 310 825 5095; fax: +1 310 206 4584.

E-mail address: [sdevaskar@mednet.ucla.edu](mailto:sdevaskar@mednet.ucla.edu) (S.U. Devaskar).

Lipid metabolism is closely controlled at the cellular level by classical transcriptional regulatory components of cholesterol metabolism, SREBP and Liver X Receptor (LXR) along with members of noncoding RNAs consisting of microRNAs (*miRNAs*) as one class of them [14,15]. *miRNAs* are RNAs of 20–25 nucleotides size and are recognized as negative post-transcriptional regulators of genes. By binding to the complementary 3'- untranslated region (UTR) of messenger RNAs, microRNAs degrade target mRNAs or block translation. Several *miRNAs* are functionally involved in regulating the lipid metabolism, such as *miR-33*, *miR-122*, *miR-27a/b*, *miR-378*, *miR-34a* and *miR-21*. Of these *miRNAs*, *miR-122* is expressed with high prominence in developing and adult livers and has been reported to be a key regulator of hepatic fatty acid and cholesterol metabolism [15]. In addition, *miR-122* has various other regulatory roles related to cellular senescence and stress response, circadian regulation of hepatic genes, iron metabolism, and propagation of specific hepatitis producing viruses. While *miR-122* promotes hepatic fatty acid synthesis in adult livers, in the IUGR offspring, when exposed to postnatal caloric restriction or of the female sex, there is a protection against developing adult onset obesity with the metabolic syndrome phenotype. Whether hepatic *miR-122* expression and its role in lipid biosynthesis are modified in response to IUGR with or without postnatal caloric restriction, or by the female sex, remains unexplored. Our previous investigations in the female IUGR offspring revealed perturbed milk and food intake patterns [16] suggestive of hypothalamic involvement [16]. Further, while we have previously observed that the metabolic phenotype of the male IUGR offspring with postnatal caloric restriction displays circadian dysregulation [17], the perturbed expression of hypothalamic genes including *miR-122* [18], associated with such hepatic dysregulation requires investigation. Therefore, in the present study, we hypothesized that hepatic fatty acid and cholesterol metabolism are adversely affected by reduced *miR-122* expression. This is in association with perturbed

hypothalamic circadian genes and *miR-122*, responsive to postnatal calorie and thereby growth restriction (GR) by itself, or when superimposed on prenatal calorie restriction with IUGR, particularly in the female offspring at an early stage of development. In order to test this hypothesis, we separated the effects of prenatal (IUGR) vs. postnatal (PNGR) and superimposed postnatal on prenatal calorie and thereby growth restriction (IPGR) in weanling female rats.

## 2. Materials and methods

### 2.1. In vivo studies

#### 2.1.1. Maternal Nutrition Restriction Model

Pregnant Sprague–Dawley rats received ~50% of their daily food intake beginning from gestation day 11 through day 21, causing caloric restriction during mid- to late pregnancy (~11 g/day), compared to their control counterparts who received ad libitum rat chow (~22 g/d) (Diet 7013 from Envigo, Madison, WI, USA: Energy 3.1 kcal/kg, [calories from protein 23%, from fat 18%, and from carbohydrate 59%] crude protein 18%, fat [ether extract] 6.2%, carbohydrate 45%, crude fiber 4%, neutral detergent fiber 13.6% and ash 6.2%). Both groups accessed drinking water ad libitum. At birth, the litter size was culled to six. Four groups were created by cross-fostering with control mothers (~40 g/d) rearing control pups (CON) or prenatally growth restricted pups (IUGR), and pre- and postnatal calorie restricted mothers (~20 g/d) rearing prenatally growth restricted pups (IPGR) or control pups (PNGR) (Fig. 1). At day 21, the female pups were examined soon after weaning from the mother.

#### 2.1.2. Body weight, organ weight and nose-tail length

Body weight, organ weight and nose-tail length were measured in 21-day-old animals from all four groups. The animals were first weighed and then deeply anesthetized by inhalation of isoflurane, nose-tail length was recorded and organs/tissues [brain, brown adipose tissue (BAT), pancreas, liver and skeletal muscle] were mechanically isolated and weighed individually.

#### 2.1.3. Plasma Metabolites and hormones/growth factors

Plasma insulin and leptin were quantified by double antibody radioimmunoassays (Linco Research, St. Charles, MO, USA). In addition, serum triacylglycerol, cholesterol, high-density lipoprotein (HDL), unesterified cholesterol and free fatty acids were measured by colorimetric assays. Total plasma ketone bodies were measured with a

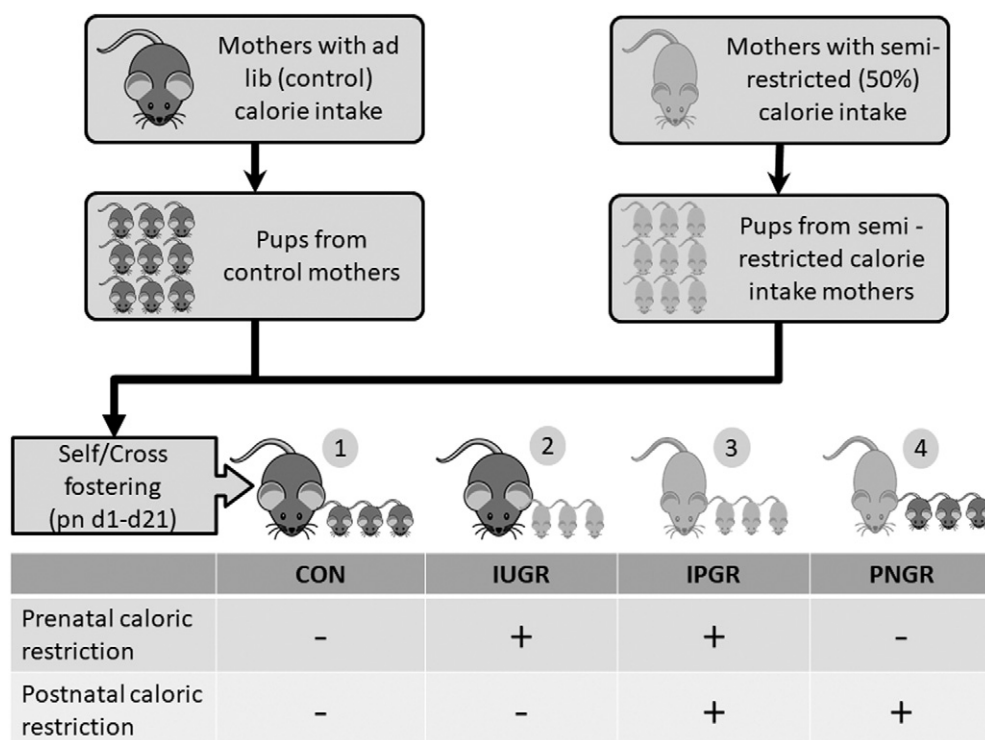


Fig. 1. Study design. Cartoon depicting the four experimental groups obtained by cross-fostering postnatal rat pups. 1) Control rats (CON), i.e. control mothers rearing control pups, 2) Intrauterine calorie restricted pups (IUGR), i.e. CON mothers rearing prenatal calorie restricted pups, 3) intrauterine and postnatal calorie restricted rats (IPGR), i.e. prenatal and postnatal calorie restricted mothers rearing prenatal calorie restricted pups, 4) postnatal calorie restricted rats (PNGR), i.e. control mothers exposed to postnatal calorie restriction rearing control pups.

commercial kit (Wako Diagnostics, Richmond, VA). Insulin-like growth factor 1 (IGF-1) measurement was conducted as previously described [19]. Briefly, serum samples were pre-extracted with acid/ethanol reagent (12.5% 2 N HCl and 87.5% ethanol), neutralized with 1 M Tris base and then diluted with assay buffer. In-house enzyme-linked immunoassays were used to measure rat IGF-1 concentrations. Ninety-six well microtiter plates were coated with capture antibody at pH 7.4, and incubated with serum samples at room temperature for 2 h. The reaction was terminated by the addition of 50  $\mu$ l of 2 N H<sub>2</sub>SO<sub>4</sub> and the absorbance was determined at 490 nm in an ELISA plate reader (Molecular Design, Sunnyvale, CA, USA). The IGF-1 assay has a sensitivity of 0.1 ng/ml. The intra-assay and inter-assay coefficients of variation were <10% in the range from 1 to 10 ng/ml.

## 2.1.4. Hepatic studies

**2.1.4.1. Western blot analysis.** Western blot analysis was performed as previously described [16]. In brief, 50  $\mu$ g of liver was homogenized in cell lysis buffer (Cell Signaling Technology, Danvers, MA, USA), and was subsequently separated on SDS-PAGE, and electro-blotted onto nitrocellulose membranes. The membranes were incubated with Mouse fatty acid synthase (FAS) and acetyl CoA carboxylase (ACC) antibodies (BD transduction laboratories, San Jose, CA, USA) overnight at 4°C. Mouse anti-vinculin (Sigma, St. Louis, MO, USA) was used as an internal loading control. The proteins were visualized in Typhoon 9410 Phosphorimager (GE Healthcare Biosciences, Piscataway, NJ, USA) by blotting with enhanced chemiluminescence (ECL) Plus detection kit (GE Healthcare Biosciences) followed by quantification in Image Quant 5.2 software (GE Healthcare Biosciences) and normalized to vinculin.

**2.1.4.2. Mitochondrial carnitine palmitoyl transferase 1 $\alpha$  (CPT1 $\alpha$ ) enzyme activity.** Fresh livers (450 mg) were isolated from CON, IUGR, IPGR and PNGR rats and placed in ice-cold mitochondria isolation buffer (300 mM sucrose, 1 mM EGTA, 5 mM HEPES, pH 7.4, 1 mg/ml BSA [20]). The livers were minced with scissors on ice and homogenized using four (up and down) strokes with a motor-driven pestle rotating at 550 rpm. The homogenates were centrifuged at 600 $\times$ g for 12 min. The pellets were then discarded and the supernatants collected and centrifuged at 6800 $\times$ g for 12 min. The supernatants were removed and the pellets re-suspended in mitochondria isolation buffer and centrifuged again at 12,000 $\times$ g for 12 min. The supernatants were discarded and the pellets re-suspended again in mitochondria isolation buffer. After centrifugation at 12,000 g for 12 min, the final pellets were re-suspended in a 1 ml mitochondria isolation buffer without EGTA. Palmitoyl-CoA was incubated with 100  $\mu$ g of liver mitochondria enriched samples from four groups and 10  $\mu$ l diluted L-[methyl-<sup>3</sup>H] carnitine in assay buffer for 10 min, and 1-BuOH was used to extract the formed palmitoyl-carnitine.

**2.1.4.3. Ex vivo hepatic fatty acid oxidation.** Fatty acid oxidation measurement was undertaken as described previously with some modifications [21]. Finely minced liver slices (~0.5 mm thick, ~150 mg) from freshly harvested livers of CON, IUGR, IPGR and PNGR were placed in 25-ml glass vials fitted with center wells containing 2 N NaOH and circular filter papers. Tissues were placed at the bottom of the vials in 2 ml of Krebs-Ringer buffer (pH 7.4) with 0.4% BSA and 1  $\mu$ Ci (57 mCi/mmol) of <sup>14</sup>C-palmitate (CFA-23; Amersham Biosciences). Vials were capped with a rubber septum, and contents of the vial were gassed with 100% O<sub>2</sub> for 10 min and incubated at 37°C for 2 h on a rotatory shaker. Then, 2 ml of 6 N HCl was injected to release <sup>14</sup>CO<sub>2</sub>. To ensure adequate transfer of <sup>14</sup>CO<sub>2</sub> to the NaOH-soaked filter papers in the center wells, vials were left undisturbed overnight at room temperature. The filter papers were transferred into scintillation fluid and radioactivity assessed.

## 2.2. In vitro studies

### 2.2.1. Cell culture

The rat H4IIE (CRL-1548) hepatocyte cells (American Type Culture Collection; Manassas, VA, USA) were cultured in DMEM medium supplemented with 10% fetal bovine serum (FBS), 50  $\mu$ g/ml streptomycin, 50  $\mu$ g/ml penicillin G and 100  $\mu$ g/ml neomycin, and grown at 37°C with 5% CO<sub>2</sub>.

### 2.2.2. Serum deprivation studies

H4IIE cells were cultured in serum-free DMEM for 24 h before they were collected for analysis.

### 2.2.3. Construction of 3'-UTR reporter plasmids

PsiCHECK™-2 vector, a dual-luciferase plasmid harboring both the synthetic Firefly Luciferase (Fluc) gene (transfection control) and the synthetic Renilla Luciferase (hRluc) gene (reporter) was obtained from Promega (C8021, Madison, WI, USA). A complementary target site for the miR-122 seed sequence (5'-CAAACACCAATTGTCA-CACTCCA-3') was inserted between the XhoI-Not I restriction sites in the multiple cloning region of the 3'-UTR of the hRluc gene [22].

### 2.2.4. Luciferase reporter assay

H4IIE cells were seeded in 96-well plates containing antibiotic-free medium for 24 h. On the day of transfection, cells were washed with PBS and switched to reduced serum medium (Invitrogen, Carlsbad, CA, USA), and transfected with 100 ng/well of the

engineered miR-122-luciferase vector or empty plasmid using lipofectamine 2000. Cells were grown at 37°C and harvested after transfection for luciferase and viability assays. Firefly and Renilla luciferase activities were measured using the Dual Luciferase Assay System (Cat.No. E1980, Promega, San Francisco, CA, USA) [22]. Relative enzyme activity was expressed as a ratio of Renilla/Firefly luciferase.

### 2.2.5. Transfection of cells with miR-122 Mimic, Inhibitor (Anti-miR-122), and respective negative control RNAs

H4IIE cells were transiently transfected with miR-122 mimic (Dharmacon, Lafayette, CO, USA) or miR-122 inhibitor at two concentrations (40 nM or 60 nM, Dharmacon, Lafayette, CO, USA) or their respective negative control RNAs, using Lipofectamine 2000 reagent (Invitrogen Life Sciences, Carlsbad, CA, USA) following the manufacturer's protocol. After 24 or 48 h the cells were subjected to trypsin treatment and RNA was harvested for the subsequent Real time PCR assay.

### 2.2.6. Reverse transcription and quantitative real-time polymerase chain reaction quantification of miR-122 from liver, H4IIE cells and plasma

Liver and H4IIE cells: Small RNAs from liver or H4IIE cells were isolated with miRNeasy mini kit (Qiagen, Valencia, CA, USA). Total RNA (10 ng) was reverse transcribed using the Taq-Man miRNA reverse-transcription kit and the TaqMan miRNA assay specific for miR-122 according to the manufacturer's instructions (Applied Biosystems, Foster City, CA, USA).

Plasma: Blood samples were collected in EDTA-containing tubes (BD vacutainer plus plastic, K<sub>2</sub>EDTA) and plasma was isolated by centrifugation at 3000 g for 15 min at 4°C. Qiagen miRNeasy Mini kit (Cat #217184, Valencia, CA, USA) was used to isolate total cell free RNA from plasma with modifications. Briefly, 1 ml of QIAzol lysis reagent was added to 200  $\mu$ l of plasma followed by the same amount of chloroform, and phase separation was achieved by centrifugation at 12,000 $\times$ g for 15 min at 4°C. Total RNA was isolated from the aqueous phase by submitting through RNeasy mini spin column. Total RNA (25 ng) was reverse transcribed using the Taq-Man miRNA reverse-transcription kit and the TaqMan miRNA assay specific for miR-122 (Applied Biosystems, Foster City, CA, USA). Expression of mature miR-122 was measured by the Taqman microRNA Assay (Applied Biosystems, Foster City, CA, USA) specific for rno-miR-122 (Applied Biosystem assay #4427975/002245) and U6 snRNA (Applied Biosystem assay #4427975/001973) was used as an internal control. In addition, synthetic Ce-miR-39 (Applied Biosystem assay #4427975/000200) from *C. elegans* was used as a spike in control to normalize the relative concentration of plasma microRNA [23,24].

### 2.2.7. Reverse transcription and quantitative real-time polymerase chain reaction quantification of fatty acid metabolism gene transcripts and miR-122 targeted mRNAs

Total RNA from liver or H4IIE cells was extracted by using an RNAeasy mini kit (Qiagen, Valencia, CA, USA). First-strand cDNA was synthesized from 1  $\mu$ g of DNase-treated total RNA using Superscript II reverse transcriptase (Invitrogen Life Technologies, Carlsbad, CA, USA), as previously described [16]. Primers and Taqman probes for detection of metabolism and miR-122 targeted genes are listed in Table 1A. Taqman probes were labeled with 5'-end fluorescent dye 6-carboxyfluorescein (FAM) and 3'-end fluorescent dye N,N,N',N'-tetramethyl-6-carboxyrhodamine (TAMRA) (Applied Biosystems, Foster City, CA, USA). Taqman PCR was carried out using an ABI prism 7700 sequence detector (Applied Biosystems, Foster City, CA, USA) and glyceraldehyde-3-phosphate dehydrogenase (GAPDH) (Applied Biosystems, Foster City, CA, USA) was used as the internal control. Relative quantification of PCR products was based on value differences between the target and GAPDH using the comparative Ct method, as previously described [16].

### 2.2.8. Hypothalamic studies

For these studies, only two experimental groups (CON and IPGR) were selected for analyses.

**2.2.8.1. Microarray-based expression profiling of hypothalamus.** Microarray Gene expression profiling was performed using the Affymetrix GeneChip Rat ToxFX1.0 Genome Arrays (Affymetrix, Santa Clara, CA, USA). Total RNA was extracted from hypothalamus using the QIAGEN miRNeasy Mini kit (Qiagen, Hilden, Germany). The yield and RNA purity were determined spectrophotometrically (NanoDrop, Wilmington, DE, USA) and by formaldehyde-agarose gel electrophoresis, as previously described [17]. Samples for array hybridization were prepared as described in the Affymetrix GeneChip Expression Technical Manual. Briefly, 1  $\mu$ g of total RNA was used to synthesize double-stranded cDNAs with a GeneChip Expression 30-Amplification Reagents One-Cycle cDNA Synthesis kit (Affymetrix, Santa Clara, CA, USA). Biotin-labeled cRNAs were then synthesized from cDNAs using GeneChip® Expression 30-Amplification Reagents for in vitro transcription (IVT) Labeling (Affymetrix, Santa Clara, CA, USA). After fragmentation, the biotinylated cRNAs were hybridized to array in a GeneChip Hybridization Oven 645 at 45°C for 16 h. The arrays were washed, stained, and scanned using Affymetrix Fluidics Station FS450 and GeneChip Scanner 3000 7G. Two independent replicated experiments were carried out for all treatments. The data was analyzed using the dCHIP software [25]. Pair-wise comparisons were made between CON and IPGR groups. Satisfactory image files were analyzed to generate probe intensity files.

Table 1A  
Primers and probes of *miR-122* target genes and other genes influenced by *miR-122* expression

	Primer	Probe
ALDO A (NM012495)	F ATGGCAACCGTCACAGCACTTCG R GACAGGAAAGTGACCCCA	CGAACAGTGCCCTGCGCT
BCKDK (NM019244)	F GCTGCCGTTTCCCT R GGCGTCTTGAGCAGCTCAG	CATTCTATGCCGCTGGACTATATCTCTGC
DGAT1 (NM053437)	F CTTTCTCTACCGGGATGTCA R CAGACACAGCTTTGGCCTTG	TCTGTGGTCCGCCAGCGAA
CPT1 $\alpha$ (NM031559)	F CACTGGCCGAATGTCAAGC R CCCAGAGCCCTGTACCAAG	ACGAAGAACATTGTGAGCGCGCTCC
PGC-1 $\alpha$ (NM031347)	F GCGCCAGCCACACTCA R TGGGTGTGGTTTGCATGGT	CTACAATGAATGCAGCGTCTTAGCACTCA
HMGR (NM013134)	F ATCAGCTGTACCATGCCGTCT R AGGCTTGTGAGGTAGAAGGTTG	ATCGGAACCGTGGTGGTGGG
FAS (NM017332)	F ACGGCATTACTCGTCCCTGTGT R GTGTCCCATGTTGGATTGGT	TTCCGCCAGAGCCCTTTGTAATTGGC

F = forward, R = reverse.

#### 2.2.8.2. Verification of microarray-based expression profiling by a quantitative RT-PCR.

First strand cDNA was synthesized from 1  $\mu$ g of DNase treated total RNA using Superscript II reverse transcriptase (Invitrogen Life Technologies, Carlsbad, CA, USA) and quantitative real time PCR was performed as previously described [16,26,27]. Primers and Taqman probes for detection of specific genes in hypothalamus were designed using Primer Express Software (Applied Biosystems, Foster, CA, USA) and are listed in Table 1B. These designed forward and reverse primers generated corresponding DNA fragments after amplification. Taqman probes were synthesized and labeled with fluorescent dye, 6-carboxyfluorescein (FAM) on the 5'-end and N,N,N',N'-tetramethyl-6-carboxyrhodamine (TAMRA) on the 3'-end (Applied Biosystems, Foster City, CA, USA). Taqman PCR was carried out using a StepOnePlus™ real-time PCR system (Applied Biosystems, Foster City, CA, USA). Real time PCR quantification was then performed using Taqman glyceraldehyde-3-phosphate dehydrogenase (GAPDH) or eukaryotic 18S rRNA (Applied Biosystems, Foster City, CA, USA) as internal controls. PCR amplifications were performed in triplicates. The amplification cycles consisted of 12

min at 95°C (hot start), followed by 40 cycles at 95°C for 30 s (denaturation), <50°C for glial fibrillary acidic protein (GFAP); 55°C for Fujimycin or FK506 binding protein 5 (Fkbp5), zinc finger containing the BTB (br-c, tk and bab) domain 16 (Zbtb16), insulin-like growth factor binding protein 3 (Igfbp3), hypocretin receptor 1 (Hcrtr1), hypocretin, Hcrtr2, bone morphogenetic protein (Bmp4), Igfbp5 and Ceacam10; 58°C for neuropeptide Y (NPY); 60°C for RNA binding motif 3 (Rbm3), agouti-related peptide (AgRP), pro-opiomelanocortin (POMC), cryptochrome circadian regulator 2 (Cry2), period circadian regulator 2 (Per2), and circadian locomotor output cycles kaput (CLOCK) over 30 s (annealing), and 72°C for 30 s (extension), using reagents from Applied Biosystems (Foster City, CA, USA). Relative quantification of PCR products were based on value differences between the target and glyceraldehyde 3-phosphate dehydrogenase (GAPDH) or 18S ribosomal RNA (rRNA) control using the comparative  $C_T$  method, as previously described [16,26,27]. In addition, *miR-122* expression was also assessed employing the same reverse transcription and PCR conditions as described above for the liver.

Table 1B  
Hypothalamic Target Genes for Real Time RT-PCR

Target Gene	Primer	Probe
Rbm3 (NM053696)	F 5'TTTGGCTTCATCACCTTCAC 3' R 5'CATCCAGGGACTCTCCATTC 3'	5'AGCATGCCTCCGATGCCATG 3'
AgRP (AF206017)	F 5'GCAGAGGTGCTAGATCCACAGAA 3' R 5'AGGACTCGTGACGCTTACAC 3'	5'CGAGTCTCGTTCTCCGCTCG 3'
Fkbp5 (NM001012174)	F 5'GAATCTGGGAGATGGACAC 3' R 5'CCTCCCTTGAAGTACACCGT 3'	5'TGACAAATGGCAGCCTGCTCCA 3'
Zbtb16 (NM001013181)	F 5'AGTGAATGGCTGTGGCAAG 3' R 5'CTACCTGTGTGAACCTGT 3'	5'CAAGCACCAGCTGGAGACGCA 3'
NPY (M20373)	F 5'AATCTCATCCAGACAGAGATATGG 3' R 5'CATTTCTGTGCTTTCTCTCATTAAGA 3'	5'AAGAGATCCAGCCTGAGACACTGATTCA3'
Igfbp3 (NM012588)	F 5'TTCCATCCACTCCATTCAA 3' R 5'GGCAGGGACCATATTCTGTCT 3'	5'TGGCTGTCCCTAGCCTGGCC 3'
Hcrtr1 (NM013064)	F 5'ACAACCTCTCAGTGGCAA 3' R 5'GACTTGTCTCTGGCAGAGGA 3'	5'CTGCTGCCTGCCTGGTCTGG 3'
Hypocretin (NM013179)	F 5'ATACCATCTCTCCGATTGC 3' R 5'GCCAGGGAACCTTTGTAG 3'	5'TCCCTGAGCTCCAGACACCATGA
Hcrtr2 (NM013074)	F 5'CTCTGGTGACAGACAGATTCC 3' R 5'TTTATCTCAGCAGCGACAGC 3'	5'AAATGGAAGCAGCCGACGCC 3'
POMC (AH002232)	F 5'ATAGACGTGTGGAGCTGGTGC 3' R 5'GCAAGCCAGCAGGTTGCT 3'	5'CAGCCAGTGCCAGGACCTCACCAC 3'
Bmp4 (NM012827)	F 5'CCGGATTACATGAGGATCT 3' R 5'CCAGATGTTCTCTGTATGG 3'	5'CCTGAGCGTCTGCCAGCAG 3'
Igfbp5 (NM012817)	F 5'CAAGAGAAAGCAGTGAAGC 3' R 5'GGCAGCTTCTATCCACTACTT 3'	5'CCGAAACGTGGCATCTGCT 3'
Gfap (NM017009)	F 5'TTTCTCAACCTCCAGATCC 3' R 5'CTCCTTAATGACCTCGCAT 3'	5'CCGATCTCCACCGTCTTTACCA 3'
Ceacam10 (NM173339)	F 5'CTACTGCTCAGCCTCACTTT 3' R 5'CACAGCGTCTACGGTGACTT 3'	5'TGGAGCCCTCTCACCCTGCCC 3'
Cry2 (NM133405)	F 5'GGTCCGGTATTGTGATGAGT 3' R 5'CGAGTGAAGAAGTCTTGGA 3'	5'AGCCACATCCAGCTGCCTGC 3'
Per2 (NM031678)	F 5'TCGACGTAAACAGGTTGTGT 3' R 5'TCCTCTTTGGCTTCTGAGGT 3'	5'CCCAGGAAGGACTGTCTCTCTCA 3'
Clock (NM021856)	F 5'AGGCATGTACAGTTTCAGC3' R 5'CTTCTGCTGCCAGTAATA3'	5'CATGCGTGTCCGCTGCTAGC3'

List of primers and probes of hypothalamic genes targeting qPCR analysis. F = forward, R = reverse.



Table 2A  
Body weight and plasma metabolite profile of d2 females

	Birth weight (g)	TG (mg/dl)	Cholesterol (mg/dl)	HDL (mg/dl)	UC (mg/dl)	FFA (mg/dl)	Glucose (mg/dl)
CON	7.4 ± 0.1	40.1 ± 1.6	70.8 ± 1.4	9.7 ± 1.9	22 ± 1.5	10.2 ± 0.5	74.8 ± 2.5
IUGR	6.5 ± 0.1	49.8 ± 2.6*	75.8 ± 2.9	8.7 ± 1.6	26 ± 2.4	11.3 ± 0.6	73.3 ± 1.9

Body weights and plasma metabolites at day 2 in Control and IUGR female pups. N=6 in each group, \**P*<.05 compared to CON.

### 2.3. Data analysis

Data are expressed as mean ± SEM. Inter-group differences were determined by the Fisher's paired least significant difference test when ANOVA revealed significance. When only two groups were compared the Student's *t*-test was employed. Significance was achieved at *P* values ≤.05.

## 3. Results

### 3.1. Impact of early life caloric restriction on body weight, organ weight and lipid profile

Although the birth weight of female IUGR pups was 88% of CON (*P*<.05), total TG in IUGR was 1.2-fold higher compared to CON (*P*<.05). However, no significant difference was observed in plasma cholesterol (both total and UC), HDL, free fatty acids (FFA) and glucose (Table 2A) concentrations. IUGR pups caught up, thus at 21d of age, body weight was similar to that of CON (*P*>.05). In contrast to IUGR, the body weight of the other two groups remained low, i.e. IPGR was 27% and PNGR was 37% of CON (*P*<.05 each). In addition IPGR was 26% and PNGR was 35% of IUGR body weight (*P*<.05 each). No significant change was observed in nose-tail length and brain weight among the four groups of 21-day-old rats. Interestingly, IPGR and PNGR demonstrated significant decrease in BAT (20% and 23% of CON, 30% and 35% of IUGR, respectively, *P*<.05 each) (Table 2B). A significant reduction in pancreatic weight was observed in IPGR and PNGR (both were 20% of CON and IUGR, respectively, *P*<.05 each) (Table 2B). Similarly, liver weight of IPGR and PNGR were both 35% of CON and 37% of IUGR (*P*<.05 each) (Table 2B). Substantial decrease was also observed in skeletal muscle weight of IPGR and PNGR groups (both 29% of CON and 25% of IUGR, *P*<.05 each) (Table 2B). However, no significant differences in any organ weights were observed between CON and IUGR groups.

### 3.2. Influence of early life caloric restriction on plasma biomarkers

Various plasma metabolites were measured in four 21-day-old experimental groups. Plasma glucose concentration was no different between CON and IUGR. In contrast, significant decrease was observed in IPGR and PNGR rats compared to CON (*P*<.05 each). Plasma insulin observed in IPGR was 60% of CON (*P*<.05) and 43% of IUGR (*P*<.05). Similarly, plasma insulin in PNGR was 80% of CON (*P*<.05) and 57% of IUGR (*P*<.05). Plasma leptin concentration measured in IUGR was 1.8-fold higher compared to CON (*P*<.05), while being undetectable in IPGR and PNGR (Table 2C). In addition, plasma IGF-1 concentrations

Table 2B  
Body & Organ weights and Length of d21 females.

	CON (6)	IUGR (6)	IPGR (6)	PNGR (6)
Body Weight (g)	55.2 ± 0.9	57.2 ± 0.8	14.8 ± 0.4**	20.2 ± 0.3**
N-T Length (cm)	18.5 ± 0.2	18.8 ± 0.2	15.2 ± 0.2	14.8 ± 0.3
Brain (g)	1.4 ± 0.01	1.3 ± 0.02	1.2 ± 0.01	1.2 ± 0.01
BAT (g)	0.3 ± 0.01	0.2 ± 0.02	0.06 ± 0.00**	0.07 ± 0.01**
Pancreas (g)	0.2 ± 0.02	0.2 ± 0.02	0.04 ± 0.00**	0.04 ± 0.00**
Liver (g)	2.0 ± 0.1	1.9 ± 0.1	0.7 ± 0.02**	0.7 ± 0.02**
Skeletal muscle (g)	0.7 ± 0.03	0.8 ± 0.1	0.2 ± 0.02**	0.2 ± 0.02**

Body and Organ weights and nose-tail Length of 21d females from all four groups. N=6 in each group, \**P*<.05 compared to CON, \*\**P*<.05 compared to IUGR. (N-T = nose-tail).

were no different between IUGR and CON, but reduced in both the IPGR and PNGR groups vs. both the IUGR and CON groups (Table 2C). Plasma total ketone bodies on the other hand were 2.9-fold higher in IUGR compared to CON (*P*<.05), while IPGR and PNGR revealed 7.2 fold and 8.0 fold increase compared to CON (*P*<.05 each) and 2.4 fold and 2.7 fold increase when compared to IUGR (*P*<.05 each; Table 2C). Plasma TG in IUGR was similar to CON, in contrast, IPGR and PNGR revealed significantly reduced TG compared to CON (*P*<.05 each) and IUGR (*P*<.05 each). Plasma HDL demonstrated a similar pattern, with IPGR demonstrating 14% and 16% of CON (*P*<.05) and IUGR (*P*<.05), and PNGR being 16% and 15% of CON (*P*<.05) and IUGR (*P*<.05) respectively (Table 2C). While free fatty acids were increased by 45% in IUGR and IPGR, with a trend towards a reduction in PNGR vs. CON, no significant inter-group changes were seen with total and UC Cholesterol concentrations (Table 2C).

### 3.3. Hepatic fatty acid metabolism during early life caloric restriction - IPGR and PNGR revealed increased fatty acid oxidation and decreased fatty acid synthesis

In order to determine the energy utilization among caloric restricted groups we measured the expression of genes involved in lipid metabolism. Peroxisome proliferator activator receptor (PPAR)γ co-activator 1α (PGC-1α), the critical transcription factor of fatty acid oxidation in IPGR and PNGR was 3.5–3.6 fold higher than CON (*P*<.05 each), and 2.6–2.7 fold higher in IPGR and PNGR than IUGR (*P*<.05 each) (Fig. 2A). Consistently, CPT-1α, the rate limiting enzyme of fatty acid oxidation, that transports FAs from cytosol to mitochondria, was 3.2 fold and 2.7 fold higher than CON (*P*<.05 each) and IUGR (*P*<.05 each) respectively (Fig. 2B). CPT-1α enzyme activity using palmitoyl-CoA as the substrate was also enhanced in IPGR and PNGR compared to CON and IUGR (Fig. 2C). Simultaneously, fatty acid oxidation rate in liver explants was significantly increased as well in IPGR and PNGR, as both of them were 1.5-fold higher than CON (*P*<.05 each) and 2-fold higher than IUGR (*P*<.05 each) (Fig. 2D).

In contrast, FAS, one of the key enzymes that mediates fatty acid synthesis was significantly decreased in IPGR (7% of CON) and PNGR (7% of CON, *P*<.05 each), (8% and 9% of IUGR respectively, *P*<.05 each)

Table 2C  
Plasma hormone/growth factor and metabolite concentrations in d21 females

	CON	IUGR	IPGR	PNGR
IGF-1 (ng/ml)	318 ± 39.3	352 ± 29.3	27.2 ± 2.7**	32.2 ± 5.4**
Insulin (ng/ml)	0.5 ± 0.04	0.7 ± 0.07*	0.3 ± 0.01**	0.4 ± 0.02#
Leptin (ng/ml)	5.3 ± 0.3	9.6 ± 1.2*	ND	ND
Glucose (mg/dl)	153.3 ± 8.7	137.3 ± 21.0	89.2 ± 7.8*	101.5 ± 4.4
TG (mg/dl)	38.0 ± 2.7	43.5 ± 5.0*	12.7 ± 1.9**	11.3 ± 1.3**
HDL (mg/dl)	42.2 ± 3.4	36.8 ± 13.7	5.7 ± 0.3*	5.5 ± 0.3*
FFA (mg/dl)	6 ± 0.4	8.5 ± 2.7	8.7 ± 1.0	3.5 ± 0.3
Cholesterol (mg/dl)	122.2 ± 5.6	125 ± 20.0	121.3 ± 28.7	181.3 ± 13.2
UC (mg/dl)	40.5 ± 1.7	41.8 ± 5.9	45.2 ± 9.4	62.75 ± 4.4
Ketone bodies (plasma) (μmol/L)	163.1 ± 28.0	480.4 ± 26.7*	1171.6 ± 77.7**	1303.8 ± 135.6**

FFA – free fatty acids, TG – triglycerides, HDL – high density lipoproteins, TC – total cholesterol and UC – unesterified cholesterol.

Plasma metabolite and hormone/growth factor concentrations in 21d females of four experimental groups. N=6 in each group. \**P*<.05 vs. CON, #*P*<.05 vs. IUGR.

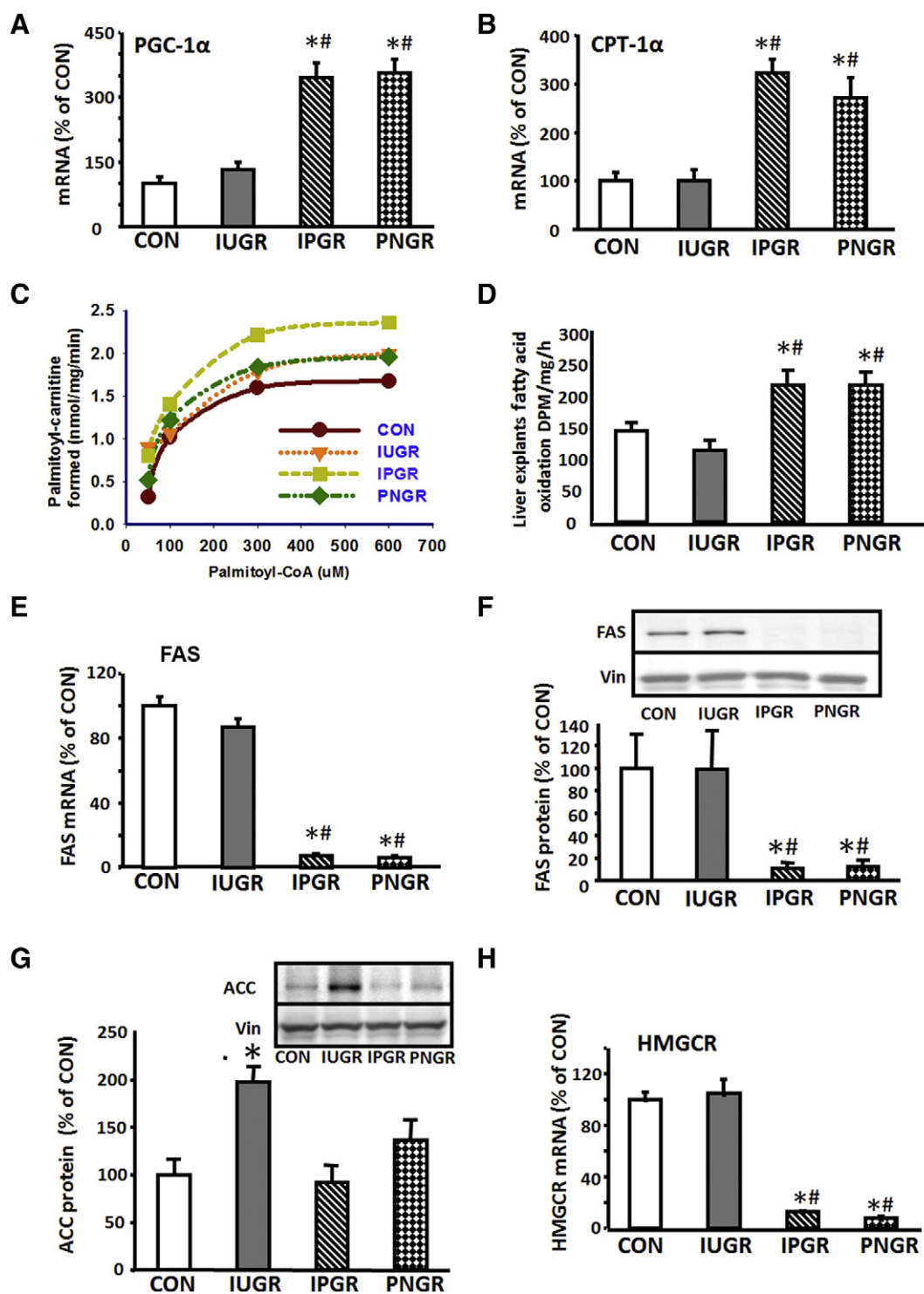


Fig. 2. In vivo and ex-vivo hepatic lipid metabolizing gene expression and function in experimental groups. **A.** PGC-1 $\alpha$  mRNA concentration was significantly increased in both IPGR and PNGR groups compared to CON and IUGR,  $^{*}P < .05$  vs. CON and IUGR in both groups, IUGR exhibited a similar PGC-1 $\alpha$  concentration to that of CON ( $P > .05$ ). **B.** CPT-1 $\alpha$  mRNA concentration was significantly increased in IPGR and PNGR groups compared to CON and IUGR,  $^{*}P < .05$  vs. CON and IUGR in both groups, IUGR exhibited a similar CPT-1 $\alpha$  concentration compared to CON ( $P > .05$ ). **C.** Mitochondrial CPT1 $\alpha$  enzyme activity is depicted in a time-dependent manner. IUGR and PNGR demonstrated higher activity when compared to CON, with IPGR exhibiting the highest activity overall. **D.** Fatty acid oxidation in IPGR and PNGR were significantly increased compared to CON and IUGR,  $^{*}P < .05$  vs. CON and IUGR in both groups. **E-F.** FAS mRNA concentration (**E**) and FAS protein (inset shows representative Western blots with vinculin as the internal control) (**F**) were both significantly decreased in IPGR and PNGR groups compared to CON and IUGR,  $^{*}P < .05$  vs. CON and IUGR for mRNA and protein in both groups, IUGR exhibited a similar FAS mRNA (**E**) and protein (**F**) concentration compared to CON ( $P > .05$ ). **G.** ACC protein was increased in IUGR vs. CON ( $^{*}P < .05$ ; inset demonstrates representative Western blots with vinculin as the internal control). **H.** HMGCR mRNA concentration was significantly decreased in IPGR and PNGR groups compared to CON and IUGR,  $^{*}P < .05$  vs. CON and IUGR in both groups, IUGR exhibited a similar HMGCR concentration compared to CON ( $P > .05$ ).

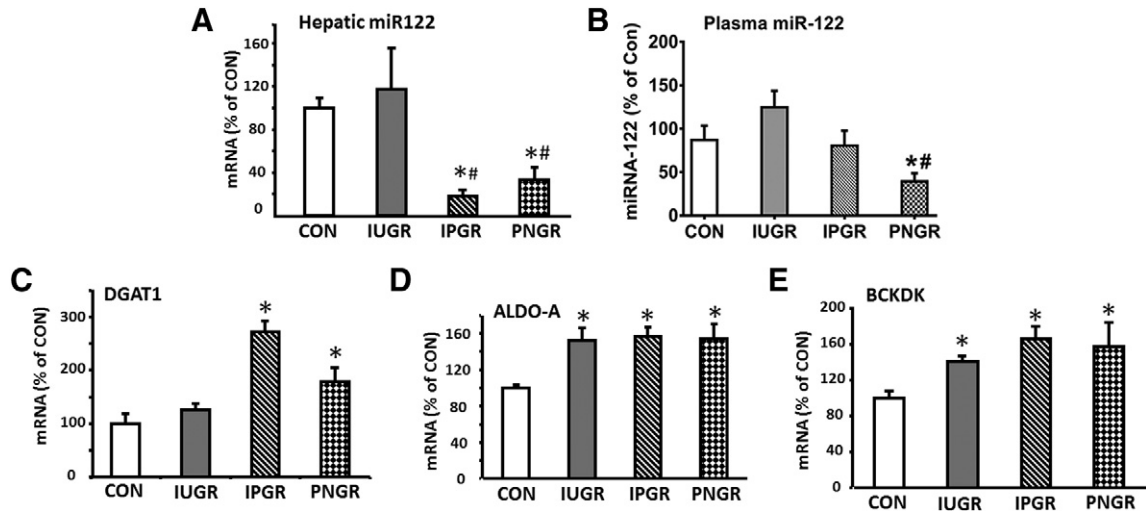


Fig. 3. Hepatic and Plasma *miR-122* mRNA and its hepatic target gene expression. **A.** Hepatic *miR-122* mRNA was significantly decreased in IPGR and PNGR compared to CON and IUGR,  $^{*}\#P<.05$  vs. CON and IUGR in both groups, *miR-122* mRNA in IUGR was similar to CON ( $P>.05$ ). **B.** Plasma *miR-122* mRNA was no different (to elevated) in IUGR and reduced in PNGR compared to CON and IPGR,  $^{*}P<.05$  vs. CON and IPGR,  $^{*}P<.05$  vs. IUGR, with  $n=6$  in each group. **C-E.** IPGR and PNGR revealed increased mRNA of *miR-122* target genes DGAT1 (**C**), ALDO-A (**D**) and BCKDK (**E**) compared to CON ( $^{*}P<.05$  each), while IUGR demonstrated a similar expression of DGAT1 (**C**) compared to CON ( $^{*}P>.05$ ), but increased ALDO-A (**D**) and BCKDK (**E**) mRNAs compared to CON ( $^{*}P<.05$  each).

(Fig. 2E). The expression of FAS protein in IPGR and PNGR were also reduced significantly (11% and 13% of CON and IUGR, respectively,  $P<.05$  each) (Fig. 2F). In contrast, ACC increased 2-fold in IUGR vs. CON ( $P<.05$ ) with no differences seen in IPGR and PNGR when compared to CON (Fig. 2G). Expression of 3-hydroxy-3-methylglutaryl-coenzyme A reductase (HMGCR), the rate limiting enzyme in cholesterol synthesis, was decreased in IPGR (13% of CON and IUGR,  $P<.05$  each) and PNGR (8% of CON and IUGR,  $P<.05$  each) (Fig. 2H).

#### 3.4. Hepatic *miR-122* expression altered in response to early life caloric restriction

*miR-122* has been shown to regulate fatty acid synthesis and fatty acid oxidation [14], thereby striking a balance in fatty acid metabolism by modifying genes such as FAS, CPT-1 $\alpha$  and HMGCR. The expression of mature *miR-122* in IPGR was 20% of CON ( $P<.05$ ) and 17% of IUGR ( $P<.05$ ), similarly, PNGR was 44% of CON ( $P<.05$ ) and 38% of IUGR ( $P<.05$ ) (Fig. 3A). The secreted *miR-122* concentrations in plasma were different from the corresponding liver *miR-122* expression, with IUGR displaying a trend towards a 1.6-fold increase and PNGR a 40% reduction ( $P<.05$ ), with no change observed in IPGR vs. CON (Fig. 3B). The decrease in hepatic *miR-122* expression in IPGR and PNGR was associated with a simultaneous increase in its reported target genes. Diacylglycerol O-acyltransferase 1 (DGAT1) was 3-fold more than in CON and 2-fold of that in IUGR (Fig. 3C), aldolase A (ALDO-A) was ~1.5 fold more in IUGR, IPGR and PNGR than that of CON ( $P<.05$  each) (Fig. 3D). Branched chain ketoacid dehydrogenase kinase (BCKDK) was ~1.4–1.7 fold greater in IUGR, IPGR and PNGR than in CON ( $P<.05$  each) (Fig. 3E).

#### 3.5. Endogenous *miR-122* reduces Renilla luciferase activity in rat H4IIE cells

We employed an experimental system of rat H4IIE hepatoma cells that previously demonstrated insulin sensitivity of the glucose and lipid metabolism [28]. Using these cells, we measured *miR-122*'s inhibitory activity on target mRNAs with the help of a dual luciferase assay system. A complementary target site for *miR-122* seed sequence was sub-cloned at the 3'-end of the *hRluc* gene (Fig. 4A). The theory being that any endogenous *miR-122* present will bind to its complementary target site of the seed sequence inserted in the 3'-

UTR of the *hRluc* gene and post-transcriptionally decrease the luciferase enzyme activity. As such a huge reduction in luciferase activity upon transfection of the constructed *hRluc* gene in H4IIE cells was observed when compared with cells transfected with the empty vector (4% compared to Control;  $P<.05$ ) (Fig. 4B). Thus, we next examined the effects of serum starvation, *miR-122* overexpression and inhibition in these H4IIE cells.

#### 3.6. Serum starvation in vitro

To mimic the in vivo chronic caloric restriction in rats, in vitro serum starvation over a shorter time-frame in H4IIE cells was undertaken. Consistent with our in vivo results, *miR-122* expression in serum starved cells was 54% of CON ( $P<.05$ ) (Fig. 5A). Simultaneously, ALDO-A, the reported target gene of *miR-122* in serum

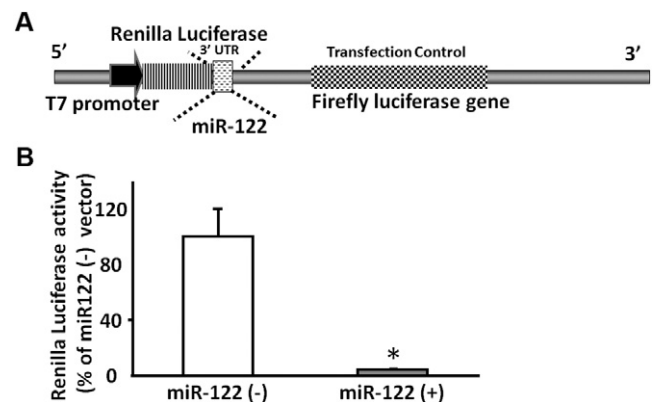


Fig. 4. In vitro study of *miR-122* functional activity. **A.** Structure of the engineered *miR-122* 3'UTR reporter plasmids: psiCHECK™-2 vector is a dual-luciferase plasmid containing both the synthetic Firefly Luciferase (Fluc) gene and the synthetic Renilla Luciferase (hRluc) gene. The complementary target sequences of *miR-122* seed sequence (5'-CAAACACCATGTGTCACACTCA3') were inserted between the XhoI-NotI restriction sites in the multiple cloning region of the 3'UTR of the hRluc gene. Functional activity of endogenous *miR-122* is reflected as the luciferase activity emanating from the reporter hRluc gene (reporter) with Fluc acting as the transfection control. **B.** The endogenous *miR-122* in H4IIE cells annealing with its complementary seed sequences inserted in the 3'UTR of the hRluc gene significantly decreased Renilla Luciferase activity, ( $^{*}P<.05$  vs. *miR-122* (-) vector),  $n=6$  in each group.



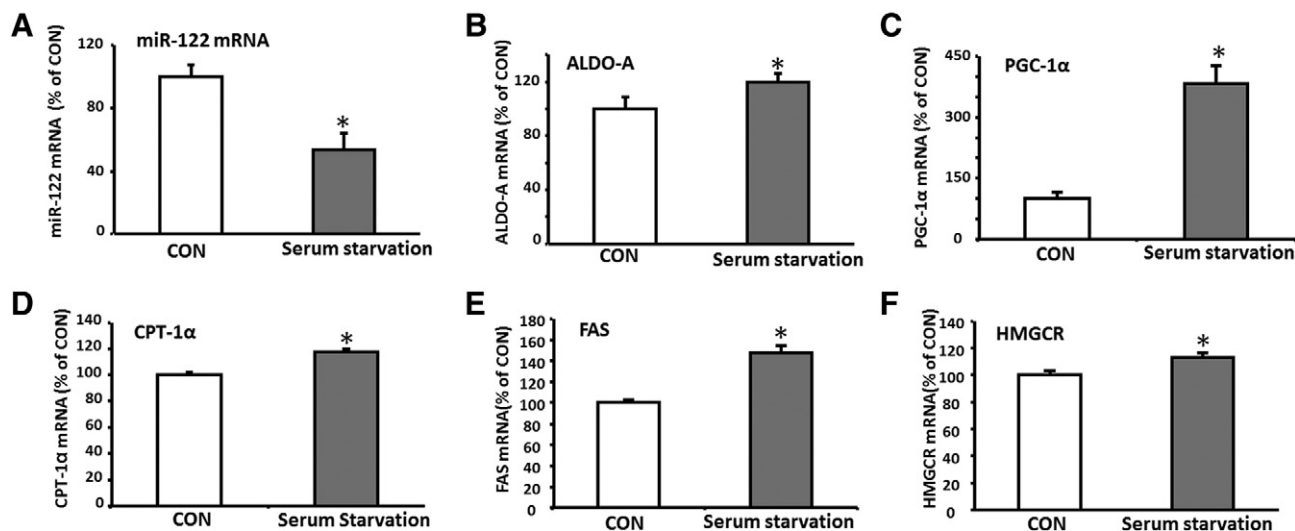


Fig. 5. In vitro serum starvation of H4IIE cells. Serum starvation of H4IIE cells for 24 h decreased *miR-122* mRNA (A) and increased *miR-122* target gene ALDO-A expression (B), fatty acid oxidation mediators PGC-1α mRNA (C) and CPT-1α (D) expression, and lipid synthesizing FAS (E) and HMGCR expression (F) compared to CON cells maintained in serum (\* $P < .05$  vs. CON). N=6 in each group and for each measurement.

starved cells was 20% more than CON ( $P < .05$ ) (Fig. 5B), PGC-1α was 3.8 fold higher in serum starved cells compared to CON ( $P < .05$ ) (Fig. 5C). In addition, serum starvation increased CPT-1α expression by 20% compared to CON ( $P < .05$ ) (Fig. 5D). PPAR-β, a potential target of *miR-122*, was also 20% higher in serum-starved cells vs. CON cells (data not shown). Contrary to the in vivo results, serum starvation in vitro in H4IIE cells increased FAS mRNA by 50% (Fig. 5E) and HMGCR mRNA by 20% compared to CON ( $P < .05$  each) (Fig. 5F).

### 3.7. *miR-122* overexpression in vitro using *miR-122* mimic

Transfection efficiency of *miRIDI*AN mimic (Dharmacon) in H4IIE cells was evaluated using a transfection control construct containing the dye Dy-547 (Fig. 6A). The transfection efficiency achieved was >90% (Fig. 6B). Transient transfection of *miR-122* mimic at 15 nM, 25 nM and 40 nM doses over 24 h resulted in a dose-dependent increase in *miR-122* expression. Based on these results, 40 nM was used as the final dose in subsequent experiments, where *miR-122* expression increased by 2.4 fold ( $P < .05$ ) compared to the transfection negative control (CON) (Fig. 6B). Consistently, *miR-122* mimic decreased ALDO-A mRNA (80% of CON,  $P < .05$ ) (Fig. 6C) and BCKDK mRNA (50% of CON,  $P < .05$ ) concentrations (Fig. 6D). HMGCR and FAS expression increased in response to *miR-122* overexpression by 40% and 20% ( $P < .05$  each) respectively (Fig. 6E,F), but PGC-1α and CPT-1α expression were also increased by 3.4-fold and 30% respectively, ( $P < .05$  each) (Fig. 6G,H).

### 3.8. Inhibition of *miR-122* expression in vitro using *miR-122* inhibitor

Inhibition of *miR-122* by an inhibitor decreased endogenous *miR-122* expression to 47% of CON ( $P < .05$ ) (Fig. 7A), which was associated with an increase in ALDO-A expression by 20% vs. CON ( $P < .05$ ) (Fig. 7B). Inhibition of *miR-122* expression also decreased HMGCR mRNA (82% of CON,  $P < .05$ ) (Fig. 7C), and FAS mRNA (86% of CON) (Fig. 7D). However in contrast to our in vivo observations, reduced *miR-122* in vitro was associated with decreased PGC-1α expression (74% of CON,  $P < .05$ ) (Fig. 7E) with no change in CPT1α mRNA (90% of CON,  $P > .05$ ) (Fig. 7F).

A summary of all the in vivo and in vitro experimental observations involving directional perturbations is provided in Table 3.

### 3.9. Identification of hypothalamic genes and their transcripts

Microarray analysis of DNA reverse transcribed from extracted hypothalamic RNA obtained from two groups, namely the CON and IPGR revealed significant changes in various genes. An increase in the top 11 genes with a decrease in the bottom 12–26 genes in IPGR vs. CON is seen (Fig. 8A). Some of these changes were further validated by RT-PCR and a significant increase in *Rbm3*, *AgRP*, *Fkbp5*, *Zbtb16*, *Npy*, *Igf1bp3* and *Hcrt1* was observed in IPGR vs. CON ( $P < .002$ ). In contrast, while no change was seen with *Hcrt*, *Hcrt2* and *Igf1bp5*, a reduction in *Pomc*, *Bmp4* (trending down), *GFAP* and *Ceacam 10* ( $P < .002$ ) was observed (Fig. 8B). Next, we focused on circadian genes in particular, which revealed an increase in *Cry1&2* and *Per2&3* transcripts with the *CLOCK* transcript being equivocal in IPGR vs. CON (Fig. 8C). These observations were also validated by RT-PCR in the case of *Cry2*, *Per2* and *CLOCK* transcripts ( $P < .006$ ) (Fig. 8D). Further, similar to the liver, we observed a reduction in *miR-122* expression in the IPGR vs. the CON group (Fig. 8E), a gene that was undetectable by microarray analysis.

## 4. Discussion

We have for the first time, demonstrated changes in postnatal hepatic and plasma *miR-122* expression in the context of genes mediating fatty acid synthesis and oxidation, thereby regulating lipid metabolism. Our four experimental groups allowed distinction between IUGR exposed to adequate postnatal nutrition with catch-up growth from the poorly postnatal nourished PNGR and IPGR groups. The latter two groups demonstrated reduced body, liver, skeletal muscle, pancreas and brown adipose tissue weights at 21d of age. The IUGR group, at birth had high circulating triglyceride concentrations that remained so until 21d of age, along with elevated fatty acids (trend seen), insulin and leptin concentrations. These changes being consistent with the IUGR female being insulin and leptin resistant with dyslipidemia, all signs of early emergence of obesogenic tendencies and the metabolic syndrome. In contrast, the PNGR and IPGR groups displayed low body, liver, skeletal muscle, pancreas and brown adipose tissue weights with reduced plasma IGF-1, insulin, leptin, glucose, triglycerides and HDL cholesterol concentrations. These findings being consistent with early emergence of insulin and leptin sensitivity. Thus similar to the male counterpart [17], female IUGR offspring are prone for maladaptation when exposed to a normal postnatal diet following prenatal diet restriction,



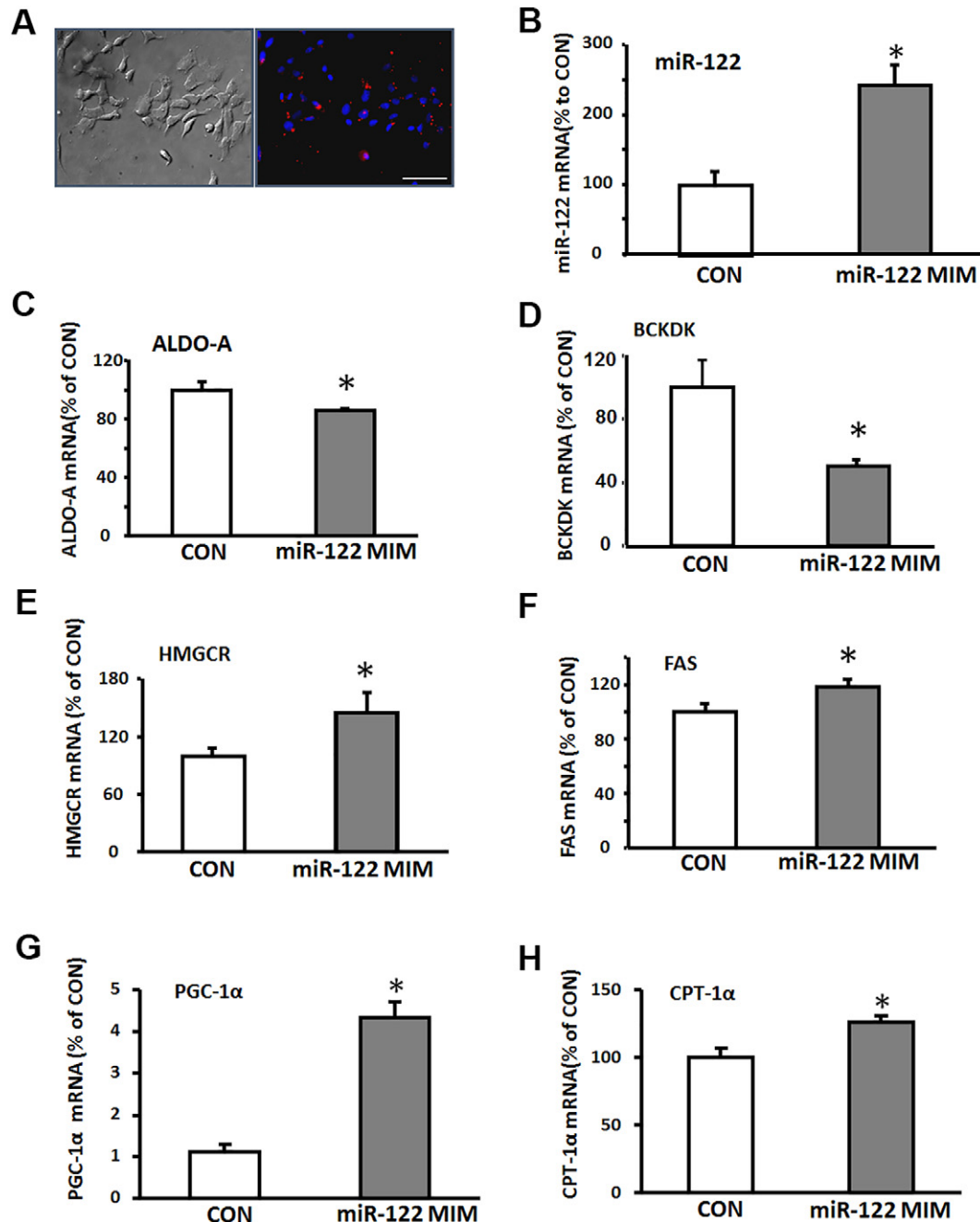


Fig. 6. In vitro over-expression of *miR-122* in H4IIE cells. Normarski imaged photomicrograph of H4IIE cells employed for transfection of *miR-122* related sequences (A, left panel). Representative photomicrograph shows transfection efficiency of miRIDIAN mimic (Dharmacon) using its transfection control plasmid containing dye Dy-547 (seen as red staining in A, right panel). Transfection of *miR-122* mimic at 40 nM versus scrambled sequences (CON) increased *miR-122* mRNA expression,  $*p < 0.05$  versus CON (B), and consequently decreased target genes ALDO-A (C) and BCKDK (D) gene expression ( $*p < 0.05$  versus CON), while increasing HMGR (E), FAS (F) and PGC-1 $\alpha$  (G) and CPT-1 $\alpha$  (H) mRNAs ( $*p < 0.05$  versus CON). N=6 for each group and for each measurement. Normarski imaged photomicrograph of H4IIE cells employed for transfection of *miR-122* related sequences (A, left panel). Representative photomicrograph shows transfection efficiency of miRIDIAN mimic (Dharmacon) using its transfection control plasmid containing dye Dy-547 (seen as red staining in A, right panel). Transfection of *miR-122* mimic at 40 nM vs. scrambled sequences (CON) increased *miR-122* mRNA expression,  $*p < 0.05$  vs. CON (B), and consequently decreased target genes ALDO-A (C) and BCKDK (D) gene expression ( $*p < 0.05$  vs. CON), while increasing HMGR (E), FAS (F) and PGC-1 $\alpha$  (G) and CPT-1 $\alpha$  (H) mRNAs ( $*p < 0.05$  vs. CON). N=6 for each group and for each measurement.

creating a mismatch in their nutritional environments. In contrast, a match of the intra-uterine and postnatal nutritional environments as encountered by the IPGR led to a lean and insulin/leptin sensitive phenotype, all emerging as early as in the weaning period of life.

In this phenotypic backdrop, exploration of hepatic *miR-122* expression revealed normalcy in the IUGR reflected so with a tendency towards elevation in plasma concentrations. Subsequently, a decrease

of *miR-122* was seen in PNGR and IPGR livers reflected so in the plasma concentrations in the case of PNGR, while the IPGR plasma concentrations were no different from CON. Plasma *miR-122* has a translatable value to human infants with the potential of serving as a biomarker for prenatal vs. postnatal nutritional mismatch, where in the IUGR and PNGR groups that experience such a mismatch, the concentrations were perturbed. IUGR's elevation in plasma

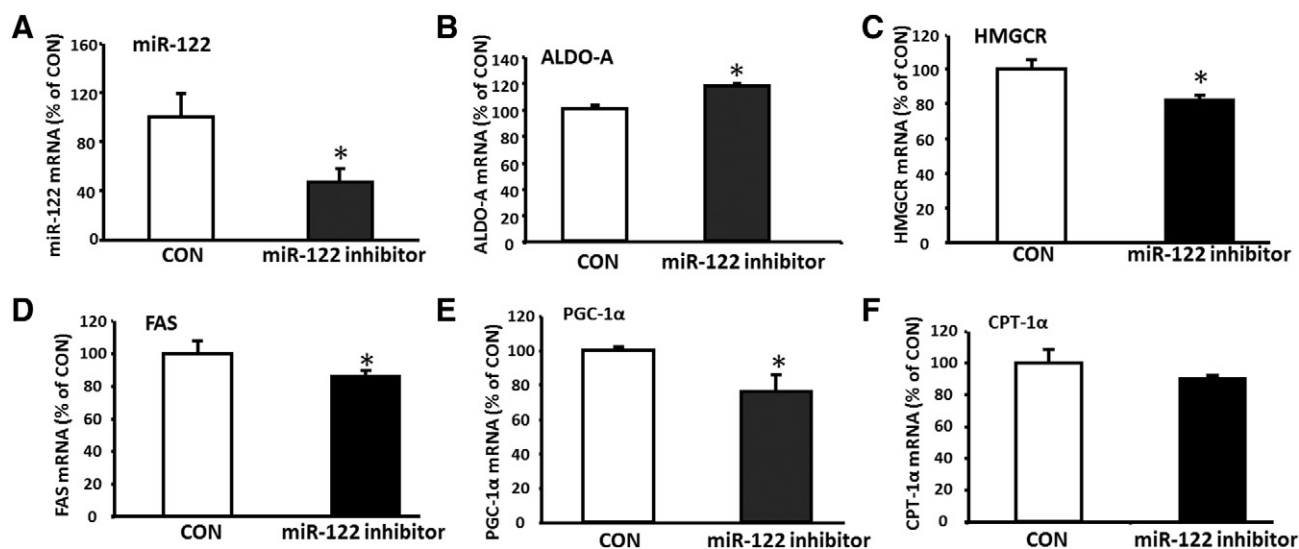


Fig. 7. In vitro inhibition of *miR-122* in H4IIE cells. Transient transfection of *miR-122* stem loop inhibitor vs. empty vector (CON) decreased endogenous *miR-122* mRNA. \* $P < 0.05$  vs. CON, (A) and simultaneously increased *miR-122* target gene ALDO-A mRNA (B), \* $P < 0.05$  vs. CON. Specific inhibition of *miR-122* decreased HMGR (C), FAS (D) and PGC-1 $\alpha$  (E) mRNAs, \* $P < 0.05$  vs. CON for each of them, while not affecting CPT-1 $\alpha$  mRNA (F,  $P > 0.05$ ).  $N = 6$  for each group and each measurement.

concentrations reflecting the catch-up growth experienced by the liver, while the reduction in PNIGR reflecting the reduction in liver size (weight). In contrast, in CON and IPGR where a perinatal nutritional match exists, the plasma *miR-122* concentrations appeared similar, despite a reduction in the IPGR's liver size. Interestingly, a positive correlation was previously observed between plasma FFA and *miR-122* concentrations [29]. Previously FFA have been observed to up-regulate the expression of hepatic *miR-122* in mouse or human hepatocellular carcinoma derived cell lines in a retinoic acid receptor-related orphan receptor- $\alpha$  (ROR $\alpha$ ) dependent manner [29], thereby enhancing the secretion of *miR-122* into the plasma. Plasma *miR-122* influences the lipid metabolism of peripheral non-hepatic tissues, thereby linking hepatic with peripheral tissue lipid metabolism. In our present study, the increased trend in plasma FFA concentrations observed in IUGR and IPGR groups may be commensurate with the increase in IUGR and IPGR plasma *miR-122* concentrations. The difference between IUGR and IPGR being the reliance of the former on an adequate supply of glucose, while the latter is dependent on ketones as a fuel supply. The PNIGR group on the other hand unlike IPGR, revealed a lower trend in plasma FFA concentrations along with reduced plasma *miR-122* concentrations.

The reduction in hepatic *miR-122* concentrations in PNIGR and IPGR was associated with an increase in transcripts of its previously determined key target genes, namely DGAT1, ALDO-A and BCKDK

[29,30]. This increase in target genes supports a functional relevance to the perturbed hepatic *miR-122* concentrations in vivo. In addition, an association with reduced FAS and HMGR expression in IPGR and PNIGR supports a functional reduction in hepatic fatty acid and cholesterol synthesis in the presence of reduced hepatic *miR-122* expression. In contrast, an increase in hepatic CPT1 $\alpha$  and PGC1 $\alpha$  expression, both mediating different processes of fatty acid oxidation, along with enhanced mitochondrial CPT1 $\alpha$  enzyme activity and fatty acid oxidation ex vivo, further supports a biological relevance seen with long chain fatty acids serving as the primary fuel (due to a low glucose supply) in PNIGR and IPGR more than in IUGR. The increase in plasma ketones in PNIGR and IPGR > IUGR, further lends credence to lipid mobilization by the process of ketogenesis. Thus, our in vivo/ex vivo female early life rodent studies provide functional relevance to the observed perturbations in hepatic and plasma *miR-122* concentrations.

To further prove the mechanistic link between *miR-122* and fatty acid metabolizing genes, we resorted to in vitro studies. To ensure adequate cellular transfection capabilities, we employed a rat hepatoma cell line, which is not completely reminiscent of a developing/postnatal liver, having arisen from an adult rat, nevertheless regenerating with cell proliferation akin to the developing liver. With these caveats, we successfully achieved >90% transfection capability of exogenous reporter DNAs, and were able to manipulate endogenous *miR-122*, either increasing or reducing it by at least 50%. These changes demonstrated functional relevance, especially with opposing changes of the target complementary sequences as assessed by the reporter assay, and at least by 20% in previously established key endogenous target genes' expression [29,30].

However, in contrast to our in vivo/ex vivo observations in early life weanling female livers, the rat hepatoma cells in vitro for the most part revealed that perturbed *miR-122* was associated with changes in FAS/HMGR and PGC1 $\alpha$ /CPT1 $\alpha$  expression that demonstrated the same directionality. Thus, elevated endogenous *miR-122* led to increased FAS/HMGR and PGC1 $\alpha$ /CPT1 $\alpha$  expression, while a reduction of *miR-122* decreased these four genes' expression. This is despite having the appropriate opposing effect on target gene transcripts such as ALDO-A/BCKDK. Hepatoma cells being cancerous in nature require increased amount of fatty acids to meet the demand of rapid proliferation. Recent findings also suggested that cancer cells can utilize both lipogenic and lipolytic pathways to procure the necessary fatty acids

Table 3  
Summary of in vivo and in vitro experiments

	<i>miR-122</i>	ALDO-A	Fatty acid synthesis	Fatty acid oxidation
PNIGR/IPGR (in vivo)	↓	↑	↓FAS ↓HMGR	↑PGC-1 $\alpha$ ↑CPT-1 $\alpha$
Serum Starvation (in vitro)	↓	↑	↑FAS ↑HMGR	↑PGC-1 $\alpha$ ↑CPT-1 $\alpha$
Inhibitor (in vitro)	↓	↑	↓FAS ↓HMGR	↓PGC-1 $\alpha$ CPT-1 $\alpha$ NC
MIMIC (in vitro)	↑	↓	↓FAS ↓HMGR	↓PGC-1 $\alpha$ ↓CPT-1 $\alpha$

Summary of in vivo results obtained in 21d females and in vitro results in H4IIE cells, respectively, showing the directionality of expression change in *miR-122*, ALDO-A, Fatty acid synthesis and Fatty acid oxidation enzymes in vivo in PNIGR/IPGR groups compared to CON, and in vitro during serum starvation, *miR-122* inhibition or overexpression (MIMIC) vs. their respective experimental controls. ↑ = increase, ↓ = decrease and NC = no change.

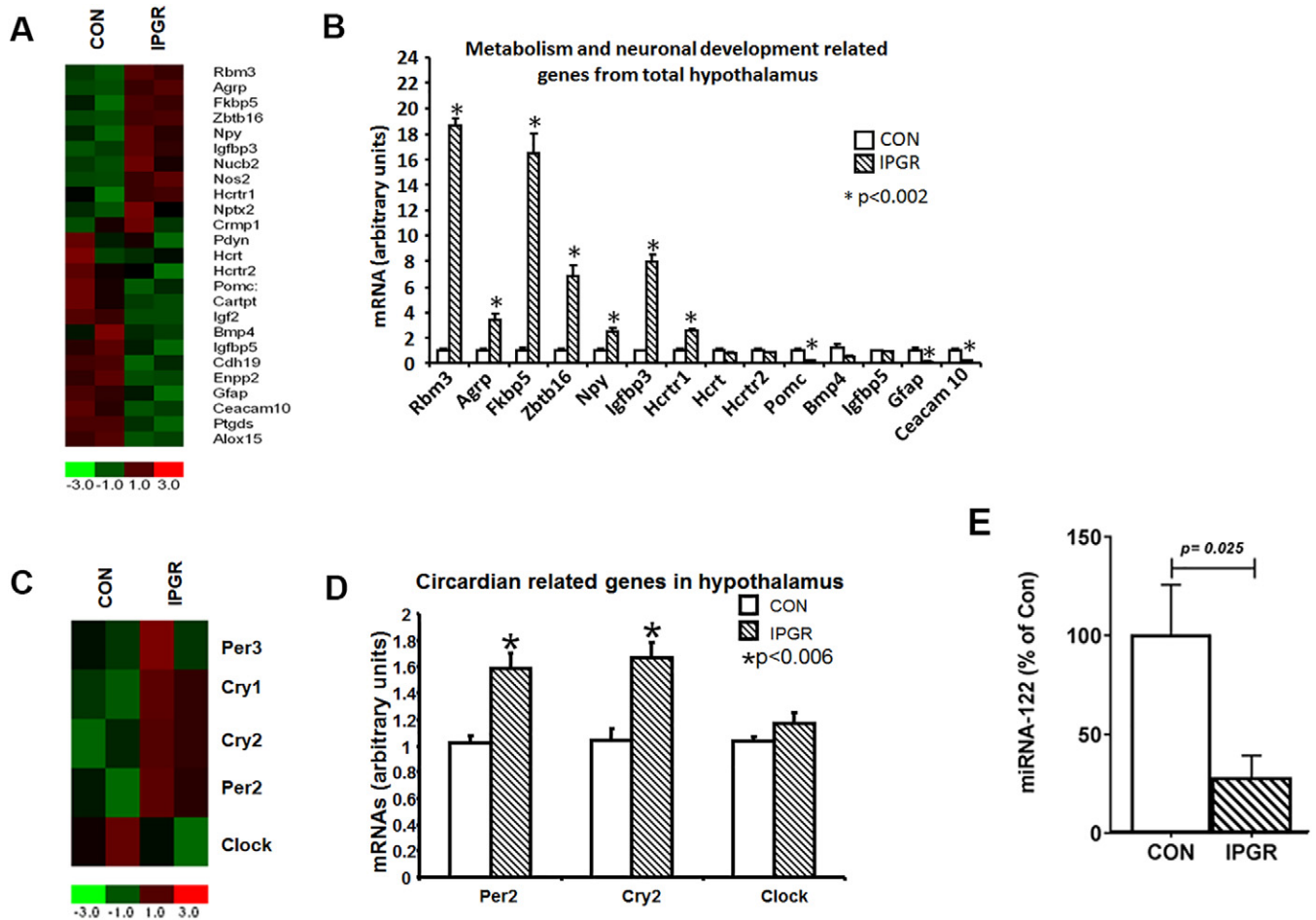


Fig. 8. Hypothalamic genes: Expression profiles of 21d CON and IPGR females. Heatmap showing the transcriptional profile of differentially expressed genes. The color code at the bottom displays fold change of gene expression (A). RT-PCR validation of expression of hypothalamic genes' expression related to metabolism in CON and IPGR female rats. Increased expression of Rbm3, AgRP, Fkbp5, Zbtb16, Npy, Igfbp3 and Hcrtr1 gene expression was observed in IPGR compared to CON, while expression of Pomc, Gfap and Ceacam 10 genes was decreased (B). Heatmap showing differentially expressed hypothalamic circadian rhythm associated genes in 21d CON and IPGR females (C). RT-PCR validation of hypothalamic genes' expression associated with circadian rhythm. The expression of Per2 and Cry2 genes was increased in IPGR compared to CON. \* $P < .05$  vs. CON (D). RT-PCR quantification of hypothalamic *miR-122* expression demonstrates a decrease in IPGR compared to CON. \* $P = .025$  vs. CON (E).  $n = 6$  in each group for each measurement.

required to fuel cellular metabolism [31,32]. These changes in gene expression thus represent a modification necessary to survive under in vitro conditions, where the culture media lacks fatty acids/ketones but rather contains high glucose concentrations (25 mM) capable of fueling intracellular lipid biogenesis and oxidation. This is unlike the in vivo conditions encountered in PNCR and IPGR, where glucose availability is low while fatty acids/ketones availability remains adequate to high.

Regardless, serum starvation studies revealed a reduction in *miR-122* along with increased PGC1 $\alpha$ /CPT1 $\alpha$  similar to the in vivo results, but unlike the in vivo observations, increased rather than decreased FAS and HMGCR expression perhaps reflecting the excessive glucose availability in the media. This increase in FAS/HMGCR expression was almost also keeping up with the increase in gene products mediating oxidation. However, when endogenous *miR-122* was genetically inhibited (rather than in response to serum starvation), ALDO-A increased as expected, and HMGCR and FAS expression was reduced as well. However, the reduction of FAS/HMGCR mRNAs was accompanied by an unexpected reduction in PGC1 $\alpha$ /CPT1 $\alpha$  expression. This change in PGC1 $\alpha$ /CPT1 $\alpha$  is unlike the PNCR/IPGR in vivo/ex vivo and the serum starvation in vitro observations.

On the contrary, upon overexpressing *miR-122* exogenously, while ALDO-A/BCKDK expression decreased as expected, FAS/HMGCR expression increased as well per expectations. However again

conflicting with the change in FAS/HMGCR expression, an increase rather than a decrease in PGC1 $\alpha$ /CPT1 $\alpha$  mRNAs was observed. Thus, it is clear that the experimental paradigm worked well based on the expected changes in key target genes' expression (ALDO-A/BCKDK), employed as positive controls. In contrast, the changes in FAS/HMGCR vs. PGC1 $\alpha$ /CPT1 $\alpha$  seem to reflect each other only in vitro supporting a complex interactive network between *miR-122* and the direct and/or indirect regulatory effect upon transcripts that mediate the balance between fatty acid/cholesterol synthesis and fatty acid oxidation.

The other observation of an ~50% perturbed *miR-122* expression being associated with only a 20% change in target mRNAs signifies that other *miRs* may be involved as well in regulating the target mRNAs involved and/or *miR-122* is engaged in post-transcriptionally regulating a network of transcripts. Thus, future studies employing hepatic RNA-sequencing may uncover these networks of target genes and pathways involved. Our current studies have attempted to uncover the role of *miR-122* in the hepatic fatty acid/cholesterol metabolism during postnatal development.

Our previous studies had revealed diurnal variations with perturbed hepatic circadian gene expression in male 21-day-old IPGR rats vs. controls [17]. Subsequently, we undertook studies in the female 21-day-old IPGR rats and observed differences in hypothalamic genes, e.g. NPY, AgRP, POMC and CART engaged in appetite control [27]. Based on these prior studies, we next deemed it essential to

undertake hypothalamic genome-wide studies of gene expression to determine the extent of changes that may be involved in regulating the hepatic lipid metabolism. While we validated our studies by RT-PCR, we were able to determine similar changes in NPY, AgRP and POMC as seen previously by us [16], serving as our experimental positive controls providing a double-check system, for our present studies. In addition, an increase in *Rbm3* (anti-apoptosis and cell proliferation, proto-oncogene), *FKbp5* (stress-related, cell proliferation/differentiation, related to type 2 diabetes and obesity), *Zbtb16* (tumor suppressor) *Igf3* (pre-diabetic, mediates cell proliferation/differentiation), *Hcrtr1* (mediates hyperphagia), *GFAP* (hypothalamic glial activation stimulates NPY/AgRP inhibiting POMC) and *Ceacam10* (mediates cell proliferation) was seen in IPGR. These changes support IPGR (PNGR superimposed on IUGR) displaying perturbed hypothalamic expression of appetite-controlling genes along with those that regulate cell proliferation/differentiation towards promoting cell survival necessary for this phenotype (PNGR-related), yet continuing to retain remnants of IUGR's propensity towards diabetes and/or obesity. Additional studies focused on circadian genes revealed an increase in specific transcripts in IPGR, namely *Per2* and *Cry2* with a tendency towards an increase in *CLOCK* expression. These findings in the hypothalamus are in keeping with prior studies demonstrating similar changes in the IPGR male livers [17], supporting a role for the hypothalamus in regulating the circadian clock relevant for hepatic metabolism. Disruption of the internal metabolic clock has a negative impact in predisposing towards metabolic disorganization subsequently [33].

Thus, the changes in the hypothalamus along with the changes in hepatic fat and cholesterol metabolic gene expression even in the female may set the stage for the adult phenotype. Along with various other regulatory mechanisms, post-transcriptional mechanisms involving various *miRs* play a key role in molding this phenotype. Previous *in vitro* studies have shown that *miR-122* reduction employing antisense methodology is associated with an increase in pAMPK [18]. In the adult hypothalamus, a reciprocal relationship was observed between *miR-122* expression and pAMPK [18], which stimulates orexigenic peptides such as AgRP and NPY [34], both of which increased in the IPGR group of our present study. Although, we did not measure pAMPK in this study, a reduction in hypothalamic *miR-122* in the IPGR vs. CON, is suggestive of increased pAMPK mediating the observed increase in AgRP and NPY. In addition, previous studies have demonstrated that IUGR reduces CPT1c in the hypothalamus, thereby reducing the central lipid sensing ability [35], perhaps explaining the noted dyslipidemia in the IUGR group in our present study.

The seeds of these phenotypes are sown prenatally, and are further modified by the postnatal nutritional environment. Thus, early determinants of aberrations in metabolic factors causing obesogenic tendencies are also evident in the female sex, having great repercussions on subsequent reproductive health with a potential effect on the next generation. In this paradigm, hepatic *miR-122* contributes towards the regulation of this ultimate phenotype of obesogenic tendencies observed in the female IUGR offspring, with partial amelioration in PNGR/IPGR.

## Acknowledgments

This work was supported by grants from the National Institutes of Health HD-41230 and HD-81206 (to SUD).

## References

- [1] Esposito K, Ciotola M, Maiorino MI, Giugliano D. Lifestyle approach for type 2 diabetes and metabolic syndrome. *Curr Atheroscler Rep*. 2008;10:523–8.
- [2] Tzanetakou IP, Mikhailidis DP, Perrea DN. Nutrition During Pregnancy and the Effect of Carbohydrates on the Offspring's Metabolic Profile: In Search of the "Perfect Maternal Diet". *Open Cardiovasc Med J*. 2011;5:103–9.
- [3] Wadhwa PD, Buss C, Entringer S, Swanson JM. Developmental Origins of Health and Disease: Brief History of the Approach and Current Focus on Epigenetic Mechanisms. *Seminars in Reproductive Medicine*. 2009;27:358–68.
- [4] Gruszfeld D, Socha P. Early nutrition and health: short- and long-term outcomes. *World Rev Nutr Diet*. 2013;108:32–9.
- [5] Larnkjaer A, Molgaard C, Michaelsen KF. Early nutrition impact on the insulin-like growth factor axis and later health consequences. *Curr Opin Clin Nutr Metab Care*. 2012;15:285–92.
- [6] Lucas A. Programming by early nutrition: an experimental approach. *J Nutr*. 1998;128:401S–6S.
- [7] Robinson S, Fall C. Infant nutrition and later health: a review of current evidence. *Nutrients*. 2012;4:859–74.
- [8] Yamada M, Wolfe D, Han G, French SW, Ross MG, Desai M. Early onset of fatty liver in growth-restricted rat fetuses and newborns. *Congenit Anom (Kyoto)*. 2011;51:167–73.
- [9] Magee TR, Han G, Cherian B, Khorram O, Ross MG, Desai M. Down-regulation of transcription factor peroxisome proliferator-activated receptor in programmed hepatic lipid dysregulation and inflammation in intrauterine growth-restricted offspring. *Am J Obstet Gynecol*. 2008;199:271 e1–5.
- [10] Dai Y, Thamocharan S, Garg M, Shin BC, Devaskar SU. Superimposition of postnatal calorie restriction protects the aging male intrauterine growth-restricted offspring from metabolic maladaptations. *Endocrinology*. 2012;153:4216–26.
- [11] Hernandez-Valencia M, Patti ME. A thin phenotype is protective for impaired glucose tolerance and related to low birth weight in mice. *Arch Med Res*. 2006;37:813–7.
- [12] Choi GY, Tosh DN, Garg A, Mansano R, Ross MG, Desai M. Gender-specific programmed hepatic lipid dysregulation in intrauterine growth-restricted offspring. *Am J Obstet Gynecol*. 2007;196:477 e1–7.
- [13] Thompson NM, Norman AM, Donkin SS, Shankar RR, Vickers MH, Miles JL, et al. Prenatal and postnatal pathways to obesity: different underlying mechanisms, different metabolic outcomes. *Endocrinology*. 2007;148:2345–54.
- [14] Esau C, Davis S, Murray SF, Yu XX, Pandey SK, Pear M, et al. *miR-122* regulation of lipid metabolism revealed by *in vivo* antisense targeting. *Cell Metab*. 2006;3:87–98.
- [15] Tsai WC, Hsu SD, Hsu CS, Lai TC, Chen SJ, Shen R, et al. MicroRNA-122 plays a critical role in liver homeostasis and hepatocarcinogenesis. *J Clin Invest*. 2012;122:2884–97.
- [16] Shin BC, Dai Y, Thamocharan M, Gibson LC, Devaskar SU. Pre- and postnatal calorie restriction perturbs early hypothalamic neuropeptide and energy balance. *J Neurosci Res*. 2012;90:1169–82.
- [17] Freije WA, Thamocharan S, Lee R, Shin BC, Devaskar SU. The hepatic transcriptome of young suckling and aging intrauterine growth restricted male rats. *J Cell Biochem*. 2015;116:566–79.
- [18] Kwon IG, Ha TK, Ryu SW, Ha E. Roux-en-Y gastric bypass stimulates hypothalamic *miR-122* and inhibits cardiac and hepatic *miR-122* expressions. *J Surg Res*. 2015;199:371–7.
- [19] Park JY, Cho MO, Leonard S, Calder B, Mian IS, Kim WH, et al. Homeostatic imbalance between apoptosis and cell renewal in the liver of premature aging Xpd mice. *PLoS One*. 2008;3:e2346.
- [20] McGarry JD, Mills SE, Long CS, Foster DW. Observations on the affinity for carnitine, and malonyl-CoA sensitivity, of carnitine palmitoyltransferase I in animal and human tissues. Demonstration of the presence of malonyl-CoA in non-hepatic tissues of the rat. *Biochem J*. 1983;214:21–8.
- [21] Cha SH, Hu Z, Chohan S, Lane MD. Inhibition of hypothalamic fatty acid synthase triggers rapid activation of fatty acid oxidation in skeletal muscle. *Proc Natl Acad Sci U S A*. 2005;102:14557–62.
- [22] Vermeulen A, Robertson B, Dalby AB, Marshall WS, Karpilow J, Leake D, et al. Double-stranded regions are essential design components of potent inhibitors of RISC function. *RNA*. 2007;13:723–30.
- [23] Fichtlscherer S, De Rosa S, Fox H, Schwietz T, Fischer A, Liebetrau C, et al. Circulating microRNAs in patients with coronary artery disease. *Circ Res*. 2010;107:677–84.
- [24] Kroh EM, Parkin RK, Mitchell PS, Tewari M. Analysis of circulating microRNA biomarkers in plasma and serum using quantitative reverse transcription-PCR (qRT-PCR). *Methods*. 2010;50:298–301.
- [25] Li C, Wong WH. Model-based analysis of oligonucleotide arrays: expression index computation and outlier detection. *Proc Natl Acad Sci U S A*. 2001;98:31–6.
- [26] Thamocharan M, Shin BC, Suddirikk DT, Thamocharan S, Garg M, Devaskar SU. *GLUT4* expression and subcellular localization in the intrauterine growth-restricted adult rat female offspring. *Am J Physiol Endocrinol Metab*. 2005;288:E935–47.
- [27] Gibson LC, Shin BC, Dai Y, Freije W, Kositamongkol S, Cho J, et al. Early leptin intervention reverses perturbed energy balance regulating hypothalamic neuropeptides in the pre- and postnatal calorie-restricted female rat offspring. *J Neurosci Res*. 2015;93:902–12.
- [28] Hectors TL, Vanparys C, Pereira-Fernandes A, Knapen D, Blust R. Mechanistic evaluation of the insulin response in H4IIE hepatoma cells: new endpoints for toxicity testing? *Toxicol Lett*. 2012;212:180–9.
- [29] Chai C, Rivkin M, Berkovits L, Simerzin A, Zorde-Khvalevsky E, Rosenberg N, et al. Metabolic Circuit Involving Free Fatty Acids, microRNA 122, and Triglyceride Synthesis in Liver and Muscle Tissues. *Gastroenterology*. 2017;153:1404–15.
- [30] Elmen J, Lindow M, Silahatoglu A, Bak M, Christensen M, Lind-Thomsen A, et al. Antagonism of microRNA-122 in mice by systemically administered LNA-antimiR leads to up-regulation of a large set of predicted target mRNAs in the liver. *Nucleic Acids Res*. 2008;36:1153–62.



- [31] Nomura DK, Long JZ, Niessen S, Hoover HS, Ng SW, Cravatt BF. Monoacylglycerol lipase regulates a fatty acid network that promotes cancer pathogenesis. *Cell*. 2010;140:49–61.
- [32] Zaidi N, Lupien L, Kuemmerle NB, Kinlaw WB, Swinnen JV, Smans K. Lipogenesis and lipolysis: the pathways exploited by the cancer cells to acquire fatty acids. *Prog Lipid Res*. 2013;52:585–9.
- [33] Potter GD, Skene DJ, Arendt J, Cade JE, Grant PJ, Hardie LJ. Circadian Rhythm and Sleep Disruption: Causes, Metabolic Consequences, and Countermeasures. *Endocr Rev*. 2016;37:584–608.
- [34] Fukami T, Sun X, Li T, Desai M, Ross MG. Mechanism of programmed obesity in intrauterine fetal growth restricted offspring: paradoxically enhanced appetite stimulation in fed and fasting states. *Reprod Sci*. 2012;19:423–30.
- [35] Puglianiello A, Germani D, Antignani S, Tomba GS, Cianfarani S. Changes in the expression of hypothalamic lipid sensing genes in rat model of intrauterine growth retardation (IUGR). *Pediatr Res*. 2007;61:433–7.